Contact processes with long range interactions

F Ginelli[1]**, H Hinrichsen**[2]**, R Livi**[3,4,5]**, D Mukamel**[6] **and A Torcini**[4,5,7]

[1] Service de Physique de l'Etat Condensé, CEA/Saclay, 91191 Gif-Sur-Yvette, France
[2] Fakultät für Physik und Astronomie, Universität Würzburg, Am Hubland, 97074 Würzburg, Germany
[3] Dipartimento di Fisica, Università di Firenze, Unitá INFM, via Sansone 1, I-50019 Sesto Fiorentino, Italy
[4] Centro Interdipartimentale per lo Studio delle Dinamiche Complesse, via Sansone 1, I-50019 Sesto Fiorentino, Italy
[5] Sezione INFN di Firenze, via Sansone 1, I-50019 Sesto Fiorentino, Italy
[6] Department of Physics of Complex Systems, Weizmann Institute of Science, Rehovot 76100, Israel
[7] Istituto dei Sistemi Complessi, CNR, via Madonna del Piano 10, I-50019 Sesto Fiorentino, Italy
E-mail: fginelli@dsm-mail.saclay.cea.fr, hinrichsen@physik.uni-wuerzburg.de, Roberto.Livi@fi.infn.it, fnmukaml@wisemail.weizmann.ac.il and alessandro.torcini@isc.cnr.it

Abstract. A class of non-local contact processes is introduced and studied using the mean field approximation and numerical simulations. In these processes particles are created at a rate which decays algebraically with the distance from the nearest particle. It is found that the transition into the absorbing state is continuous and is characterized by continuously varying critical exponents. This model differs from the previously studied non-local directed percolation model, where particles are created by unrestricted Levy flights. It is motivated by recent studies of non-equilibrium wetting indicating that such non-local processes play a role in the unbinding transition. Other non-local processes which have been suggested to exist within the context of wetting are considered as well.

J. Stat. Mech. (2006) P08008

Contents

1. Introduction

The contact process (CP) is known as a simple model for epidemic spreading that mimics the interplay of local infections and recovery of individuals [1, 2]. It is defined on a d-dimensional lattice whose sites could be either active (infected) or inactive (non-infected), denoted as '1' and '0', respectively. The model evolves random sequentially by two competing processes, namely, nearest-neighbour infections $01/10 \rightarrow 11$, and spontaneous recovery $1 \rightarrow 0$. Depending on the relative frequency of these moves the contact process displays a continuous phase transition from a fluctuating active state into an absorbing state which belongs to the universality class of directed percolation (DP) [3]–[6].

 In the present paper we investigate a generalized version of the one-dimensional contact process where inactive sites can be activated over long distances. We consider a lattice model where sites could be either active or non-active. The model evolves by random sequential updating with the following transition rates:

$$1 \rightarrow 0 \qquad \text{with rate } 1 \tag{1}$$

$$0 \rightarrow 1 \qquad \text{with rate } q/l^\alpha. \tag{2}$$

The first move corresponds to the usual local annihilation process, while the second move describes a long range process in which an inactive site which is located at a distance l from the nearest active one becomes active. The rate at which such a process takes place decays algebraically with the distance l from the nearest active site (measured in lattice site units), reflecting the long range nature of the interaction. The overall rate of this process is governed by the control parameter q, while the characteristic shape of the interaction is controlled by the exponent α. In particular, usual short range dynamics is
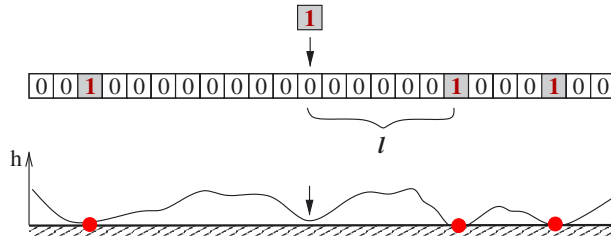
Figure 1. Long range infections in the generalized one-dimensional contact process. Any site between two active sites can be activated with a rate proportional to $l^{-\alpha}$, where l is the distance to the nearest active site. The model is motivated by the dynamics of a fluctuating interface growing on an inert substrate (see the text).

recovered in the limit $\alpha \to \infty$. In what follows we refer to this model as the α-process. Note that its definition is valid in any dimension although we are primarily interested in the one-dimensional case.

The long range contact process investigated here is motivated by recent studies of depinning transitions in non-equilibrium wetting processes [7]–[11], where one considers a fluctuating interface next to a hard-core wall. Regarding the pinned domains of the interface as active sites and unpinned domains as inactive ones, the dynamics of the fluctuating interface may be projected onto that of a contact process (see figure 1). For example, unpinning of the interface due to deposition would correspond to spontaneous recovery $1 \to 0$, while lateral growth of a pinned domain would correspond to local spreading of activity by $01/10 \to 11$. However, as unpinned regions of the interface fluctuate in the bulk they may spontaneously become pinned to the substrate far away from other binding sites. As illustrated in the figure, such a pinning effectively leads to long range infections in the corresponding contact process. Clearly, the rate for pinning will decrease as we move away from the binding site. Numerical studies of some wetting models (not shown in this work) indicate that this rate decays algebraically as $l^{-\alpha}$ with an exponent $\alpha \approx 2.6$. This motivates the postulated power law in equation (2). Nevertheless the relation between non-equilibrium wetting and the α-process should be considered as an analogy, rather than an exact mapping, because the projection neglects the internal dynamics of unpinned regions of the interface.

In recent years the contact process has also been generalized in various other ways to include long range infections [12, 13]. In these studies it is assumed that a given active site can activate *any* other site with a probability $P(k)$, which decays algebraically with the distance k as

$$P(k) \sim k^{-\alpha}. \tag{3}$$

In such models the infection can be thought of as being spread by Lévy flights [14]. Janssen *et al* solved this problem using field-theoretic renormalization group calculations [15]. The results of this analysis are in agreement with numerical simulations [16]. More recently these studies have been extended to contact processes with temporal [17] and spatio-temporal Lévy flights [18] as well as to systems with disorder [19].

The α-process studied in the present work differs from the Lévy-flight-mediated contact process. Here an inactive site can only be activated by the nearest active site.

Therefore, in one space dimension, the interaction range is effectively cut off at half the actual size of the corresponding island of inactive sites. Thus infections in the α-process are mediated by *truncated* Lévy flights, which cannot overtake other active sites. As will be shown below, this truncation changes the critical properties at the transition significantly. In particular, although both models exhibit critical exponents which vary with α, the exponents themselves are not the same. Moreover, while in the Lévy flights model the exponents become mean field like for small α [4], no such regime exists in the α-process.

In the following section we analyse the α-process using a mean field approximation as well as numerical simulations and compare it to contact processes with unrestricted Lévy flights. In section 3 we further generalize the model by taking the rate for nearest-neighbour infection to depend on the distance to the nearest active site. This rate is controlled by an additional exponent σ. The phase diagram of this generalized model, called the α–σ-process, is then studied by mean field and numerical methods. Conclusions are finally presented in section 4.

2. Analysis of the model

2.1. Mean field approximation

We now consider the α-process within a mean field approximation in terms of the density of active sites $\rho(t)$. To this end the mean field equation of the ordinary contact process has to be extended by including a term that accounts for long range infections according to equation (2). Assuming that the sites of a one-dimensional lattice are uncorrelated and independently active with probability ρ, it is easy to check that the probability for an inactive site to lie at a distance l from the nearest active site is $(1 - (1 - \rho)^2)(1 - \rho)^{2l-2}$. Summing up the contributions for all distances l, the mean field equation governing the dynamics of the density of active sites takes the form

$$\partial_t \rho = -\rho + q\rho(2 - \rho) \sum_{l=1}^{\infty} \frac{(1 - \rho)^{2l-1}}{l^\alpha} \tag{4}$$

where the first term appearing on the rhs of equation (4) corresponds to the short range annihilation process. Note that the usual DP short range activation term is given by the first term of the sum in the rhs of equation (4).

Turning the sum into an integral, the leading terms in ρ in the dynamical equation (4) may be evaluated. It is found that for $\alpha < 1$ and to leading order in ρ, equation (4) becomes

$$\partial_t \rho = r\rho + u\rho^\alpha \tag{5}$$

where (r, u) are constants and $u > 0$. Since the leading term in this equation is ρ^α, and since its coefficient is positive, the absorbing state ($\rho = 0$) is always unstable and no transition takes place for any finite q. This is also the case for $\alpha = 1$, where logarithmic corrections to the leading linear terms destabilize the absorbing phase. On the other hand, for $1 < \alpha < 2$ the leading term in the equation is the linear one. Moreover the coefficient u of the leading non-linear term is negative. This results in a continuous transition to the absorbing state which takes place at $r = 0$ corresponding to a non-vanishing rate q. Such

a phase transition belongs to a universality class different from that of the short range DP model. For example, in the stationary state the density of active sites scales as

$$\rho_{\text{stat}} \sim r^{1/(\alpha-1)}, \tag{6}$$

and hence the mean field order parameter exponent, $\beta^{\text{MF}} = 1/(\alpha - 1)$, varies continuously with α. It diverges in the limit $\alpha \to 1$. For $\alpha \geq 2$, however, the leading non-linear term is $v\rho^2$ where v is a negative constant. The mean field equation thus reduces to that of the short range DP process, and usual DP like transition is expected.

Thus

$$\beta^{\text{MF}} = \begin{cases} \dfrac{1}{\alpha - 1} & 1 < \alpha < 2 \\ 1 & \alpha \geq 2. \end{cases} \tag{7}$$

Before discussing the results of the numerical study of this model we consider a more refined mean field approximation, where the effect of the long range process on the diffusion constant is taken into account. To proceed we assume that, although the dynamical process is long range, it does not modify the usual Laplacian form of the spatial interactions, $D\nabla^2\rho$. The reason is that the infection range in the α-model is cut-off by the maximal distance to the nearest active site, making it effectively of finite range. However, as we shall see below, the effect of the α infection process is to make the diffusion coefficient D dependent on the density ρ.

In order to evaluate $D(\rho)$ we note that the infection process is cut off at length scales $l_{\text{av}} \sim 1/\rho$, which is the average distance between active particles in a system with density ρ. The mean square displacement of an infection is expected to scale as

$$\langle l^2 \rangle \sim \int_{\Lambda}^{l_{\text{av}}} \mathrm{d}l \, l^{2-\alpha} \sim \rho^{\alpha-3} + D_0 \tag{8}$$

where Λ is a cut-off due to lattice spacing from which the usual constant contribution D_0 (positive for $\alpha > 3$) to the diffusion coefficient arises. Since $D(\rho) \sim \langle l^2 \rangle$, equation (8) suggests that the effective diffusion constant diverges for $\alpha < 3$. Thus the space–time-dependent version of the mean field equation for $1 < \alpha < 2$ reads to lowest order

$$\partial_t\rho(\mathbf{x},t) = r\rho(\mathbf{x},t) + u[\rho(\mathbf{x},t)]^{\alpha} + [\rho(\mathbf{x},t)]^{\alpha-3}\nabla^2\rho(\mathbf{x},t). \tag{9}$$

For this equation, dimensional analysis yields the complete set of mean field exponents

$$\nu_{\perp}^{\text{MF}} = \beta^{\text{MF}} = \frac{1}{\alpha - 1}, \qquad \nu_{\parallel}^{\text{MF}} = 1, \tag{10}$$

where as usual $\nu_{\perp}^{\text{MF}}$ and $\nu_{\parallel}^{\text{MF}}$ are the mean field values for the spatial and temporal exponents which control the power-law divergence of correlations (respectively in space and time) at criticality.

On the other hand for $2 < \alpha < 3$ the non-linear term in the dynamical equation $u\rho^{\alpha}$ becomes $v\rho^2$ while the diffusion coefficient remains singular at $\rho = 0$. This implies that the DP regime sets up only for $\alpha \geq 3$, and not for $\alpha > 2$ as suggested by the analysis of the reaction terms alone. In particular, for $2 < \alpha \leq 3$ the lowest order mean field result reads

$$\partial_t\rho(\mathbf{x},t) = r\rho(\mathbf{x},t) + v[\rho(\mathbf{x},t)]^2 + [\rho(\mathbf{x},t)]^{\alpha-3}\nabla^2\rho(\mathbf{x},t) \tag{11}$$

and by dimensional analysis one gets

$$\nu_\perp^{\mathrm{MF}} = 2 - \frac{\alpha}{2}, \qquad \beta^{\mathrm{MF}} = \nu_\parallel^{\mathrm{MF}} = 1. \tag{12}$$

For the dynamical exponent $z = \nu_\parallel / \nu_\perp$, we obtain

$$z^{\mathrm{MF}} = \begin{cases} \alpha - 1 & 1 < \alpha < 2 \\ \dfrac{2}{4 - \alpha} & 2 \le \alpha \le 3 \\ 2 & \alpha > 3. \end{cases} \tag{13}$$

In the following we compare these values with the results of extensive numerical simulations.

2.2. Numerical results

In order to determine the critical exponents numerically, we performed Monte Carlo simulations of the one-dimensional α-process with periodic boundary conditions, starting with a fully occupied lattice. The time step $\mathrm{d}t$ of a single move in the random sequential updating procedure has been taken as $1/L$, where L is the lattice size. For models with long range interactions such simulations are difficult to perform because of strong finite size effects, which increase as $\alpha \to 1$. In the present model these finite size effects manifest themselves by sudden transitions into the absorbing state. This leads to uncontrollable fluctuations in the statistical averages. To circumvent this problem we combined finite size scaling analysis with numerical simulations. The simulations were carried out on large systems with homogeneous initial states approaching the critical point from the active phase. The critical point q_{c} and the dynamical exponent z have been determined by finite size analysis of the average absorbing time τ for an initially fully occupied lattice. At the critical point, τ is expected to scale with the system size L as

$$\tau \sim L^z. \tag{14}$$

For one-dimensional systems belonging to the DP universality class the dynamical exponent is known to be $z^{\mathrm{DP}} = 1.580\,745(10)$ [20]. We also measured the exponent $\delta = \beta / \nu_\parallel$, which is associated with the temporal decay of the density ρ of active sites at criticality. This calculation has been performed by applying the method of finite size analysis proposed by de Oliveira and Dickman [21]: whenever the system falls into the absorbing state the dynamical process is recovered by automatically resetting the system into a 'typical' active configuration. In practice, this procedure suppresses the large fluctuations which result from the abrupt transitions to the absorbing state in finite systems. A simple scaling argument shows that the stationary density at criticality should scale with the system size as

$$\rho_{\mathrm{stat}} \sim L^{-\delta z}. \tag{15}$$

Finite size analysis has been performed by averaging over 10^3–10^4 independent runs.

For $\alpha > 2.0$ the estimates of the exponent δ, obtained by finite size analysis have been compared with the standard analysis, based on the time decay of $\rho(t)$ at criticality. Usually, large fluctuations make the latter method quite inaccurate and time-consuming. In order to obtain better performances we carried out numerical simulations of large
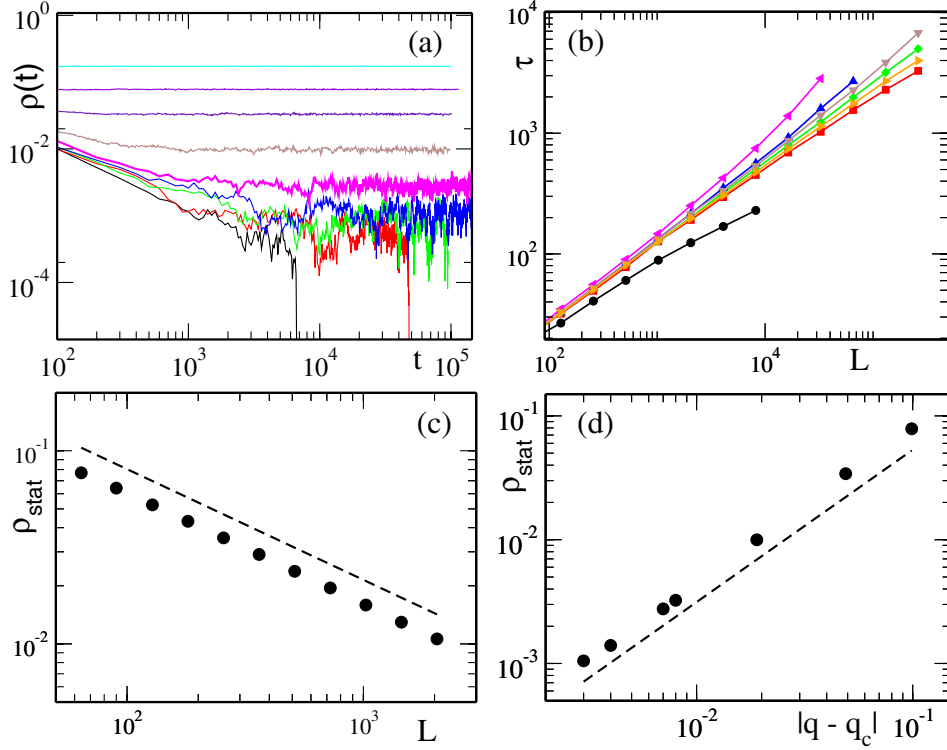
Figure 2. Results of the numerical analysis of the α-process for $\alpha = 1.5$. All plots are on a double-logarithmic scale. (a) Density of active sites $\rho(t)$ as a function of time measured for a system of size $L = 2^{20}$ starting from a fully occupied lattice. In the active phase and close to the critical value $q_c = 0.4695(5)$ (from top to bottom $q = 0.679, 0.569, 0.519, 0.489, 0.477, 0.473, 0.472, 0.471, 0.470$) finite size fluctuations yield sudden transitions to the absorbing state. (b) Finite size scaling analysis of the average absorbing time τ. From top to bottom $q = 0.475, 0.471, 0.470, 0.469, 0.468, 0.467, 0.45$. (c) Finite size scaling analysis of the stationary density ρ_{stat} (see the text). (d) Stationary density ρ_{stat} as a function of the distance from q_c. The dashed lines in panels (c) and (d) are the best fit (see table 1).

systems ($L = 2^{20}$–2^{21}) and over long time lapses (10^5–10^6 time steps), while averaging over a few different realizations. Good agreement with the predictions of finite size analysis is found.

The critical exponent β has been determined by measuring the stationary density of active sites $\rho \sim (q - q_c)^\beta$ in large systems ($L = 2^{15}$–2^{18}) for different values of q, just above q_c.

The estimated values for the exponents δ and β can be compared with the best numerical estimates of the DP exponents in one dimension, $\delta^{\text{DP}} = 0.159\,464(6)$ and $\beta^{\text{DP}} = 0.276\,486(8)$ [20]. Typical curves resulting from this numerical procedure are shown in figure 2 for $\alpha = 1.5$.

As summarized in table 1, the numerical results show a qualitative agreement with the mean field predictions. In particular, it is found that all exponents vary as α is increased up to a critical value $\bar{\alpha}$, beyond which they become consistent (within numerical error)
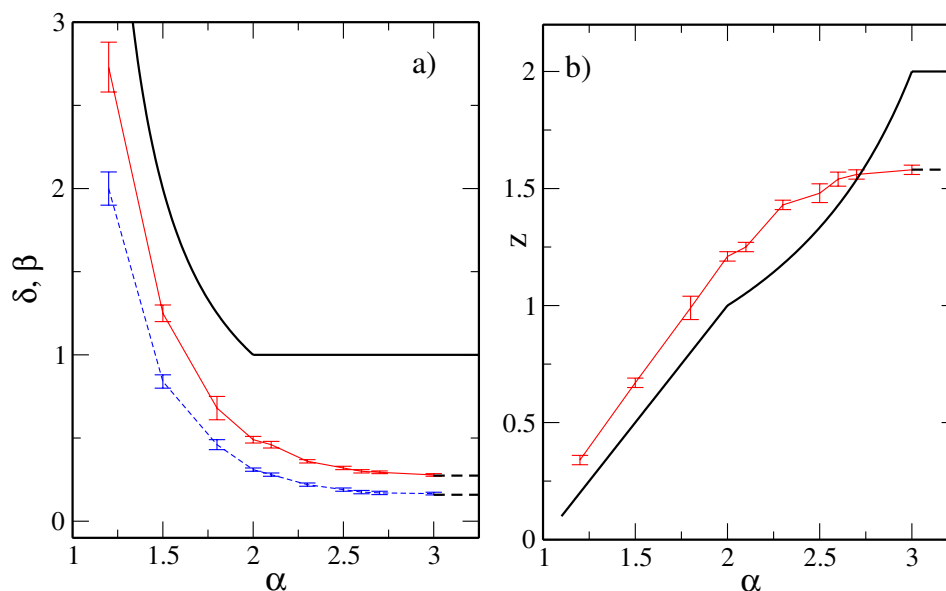
Figure 3. Comparison between numerical estimates (including error bars) and the mean field predictions for the critical exponents as a function of the control parameter α. (a) The exponents β (thin solid line), $\delta = \beta/\nu_\parallel$ (thin dashed line) and the mean field prediction (thick solid line); note that $\beta^{\mathrm{MF}} = \delta^{\mathrm{MF}}$. (b) The dynamical exponent $z = \nu_\parallel/\nu_\perp$ (thin solid line) and the mean field prediction (thick solid line). The thick dashed lines on the right of both plots mark the best numerical estimates of the DP exponents in 1D.

Table 1. Estimates of the critical points and exponents for various values of α. These values are plotted in figure 3. For comparison, mean field values are also reported.

α	q_c	z	δ	β	$\beta^{\mathrm{MF}} = \delta^{\mathrm{MF}}$	z^{MF}
1.2	0.205(3)	0.34(2)	2.0(1)	2.73(15)	5	0.2
1.5	0.4695(5)	0.67(2)	0.84(4)	1.25(5)	2	0.5
1.8	0.714(1)	0.99(5)	0.46(3)	0.68(7)	1.25	0.8
2.0	0.8592(2)	1.21(2)	0.31(1)	0.49(2)	1	1
2.1	0.9250(3)	1.25(2)	0.28(1)	0.46(2)	1	$1.0526\ldots$
2.3	1.0453(2)	1.43(2)	0.22(1)	0.36(1)	1	$1.1764\ldots$
2.5	1.1492(2)	1.48(4)	0.19(1)	0.32(1)	1	$4/3$
2.6	1.1955(2)	1.54(3)	0.175(10)	0.30(1)	1	$1.4285\ldots$
2.7	1.2381(2)	1.56(2)	0.17(1)	0.294(8)	1	$1.5384\ldots$
3.0	1.3470(2)	1.58(2)	0.166(8)	0.278(8)	1	2

with the DP values. As α approaches 1, the exponents β and δ are found to increase, while the dynamical exponent z vanishes as $\alpha - 1$. The comparison between numerics and mean field results is shown in figure 3.

Note that according to numerical results the crossover to the DP scaling regime seems to take place at $\bar{\alpha} \approx 2.7$. On the other hand, the mean field predicts that the crossover takes place in two steps: first, β and δ become DP like at $\alpha = 2$ and then the exponent z assumes its DP value at $\alpha = 3$.

2.3. Comparison with unrestricted Lévy flights

As anticipated in the introduction, it is instructive to compare the results of the α-process with those of contact processes with infections mediated by *unrestricted* Lévy flights (see [15, 16]). In the latter case three different dynamical regimes were identified:

- A mean field regime for $\alpha < 3d/2$ characterized by the critical exponents $\beta^{\mathrm{MF}} = 1$, $\nu_\perp^{\mathrm{MF}} = (\alpha - d)^{-1}$, and $\nu_\parallel^{\mathrm{MF}} = 1$, where d denotes the spatial dimension.
- A non-trivial phase for $3d/2 \leq \alpha \leq \alpha^*$ with continuously varying exponents, restricted by the additional scaling relation $\nu_\parallel - \nu_\perp(\alpha - 2d) - 2\beta = 0$.
- A DP regime for $\alpha > \alpha^*$.

Here the upper threshold for α can be expressed in terms of DP exponents by $\alpha^* = 2d + z^{\mathrm{DP}} - 2\beta^{\mathrm{DP}}/\nu_\perp^{\mathrm{DP}} \approx 3.0766(2)$. The phase structure of this model exhibits a mean field regime for $\alpha < 3d/2$ which is not present in the α-process. In this mean field regime the unrestricted Lévy flights become so long ranged that spatial fluctuations are destroyed, leading to a homogeneous distribution of active sites. In the present model, however, the long range interactions are effectively cut off at the distance to the nearest active site, and hence there is no direct communication by long range interactions between adjacent intervals of inactive sites. This restriction yields non-trivial correlations.

It is instructive to compare mean field equation (9) with the corresponding equation for unrestricted Lévy flights, which—according to the present notation—can be written as

$$\partial_t \rho(\mathbf{x}, t) = n\rho(\mathbf{x}, t) - \rho^2(\mathbf{x}, t) + D\nabla^{\alpha-1}\rho(\mathbf{x}, t). \tag{16}$$

Here $\nabla^{\alpha-1}$ is a symmetric fractional derivative, which generates unrestricted Lévy flights. Clearly, this equation has scaling properties different from those of (9). For instance, within the mean field approximation the exponent β is equal to 1. Therefore, it is probable that also in low dimensions models with truncated and unrestricted Lévy flights belong to different universality classes.

2.4. The α-process in higher dimensions

The α-process and its mean field equation can be easily generalized to $d > 1$. In this case the range, l, of the activation process of an inactive site located at i is given by the radius of the maximal 'empty' (inactive) sphere centred in i. Within the mean field approximation the average volume of the 'empty' spheres is proportional to $1/\rho$, so that the average radius of empty spheres is $\langle l \rangle \propto \rho^{-1/d}$. Moreover, the diffusion coefficient $D(\rho)$ can be easily computed by extending equation (8) to arbitrary dimension d:

$$D(\rho) \sim \rho^{((\alpha-2)/d)-1} + D_0. \tag{17}$$

Therefore, the corresponding mean field equation reads

$$\partial_t \rho = r\rho - u\rho^{\alpha/d} - v\rho^2 + D(\rho)\nabla^2\rho + \mathrm{o}(\rho^2), \tag{18}$$

where $r(q)$ vanishes at the critical point while $u(q)$ and $v(q)$ are positive constants. As in the 1D case, if $\alpha < d$ the absorbing state cannot be reached and there is no transition. On the other hand, for $\alpha > 2d$ and $d \geq 2$ a DP regime sets in, where both leading terms

in the dynamical equation and in the diffusion constant become DP like. In the range $d < \alpha < 2d$ the system displays a non-trivial transition, with continuously varying critical exponents.

In summary, the mean field exponents for $d \geq 2$ are

$$\nu_\parallel^{\mathrm{MF}} = 1, \tag{19}$$

$$\beta^{\mathrm{MF}} = \delta^{\mathrm{MF}} \nu_\parallel^{\mathrm{MF}} = \begin{cases} \dfrac{1}{\alpha/d - 1} & d < \alpha < 2d \\ 1 & \alpha > 2d \end{cases} \tag{20}$$

and

$$\nu_\perp^{\mathrm{MF}} = \frac{\nu_\parallel^{\mathrm{MF}}}{z^{\mathrm{MF}}} = \begin{cases} \dfrac{1}{\alpha - d} & d < \alpha < d + 2 \\ \dfrac{1}{2} & \alpha \geq d + 2. \end{cases} \tag{21}$$

3. Generalization of the model

3.1. The σ-process

In a recent paper we studied a different version of a contact process with long range interactions, called a σ-process [22]. In this model infections are short ranged, i.e., active sites can only activate their nearest neighbours, but the *rate* for short range infections depends algebraically on the distance m to the nearest active site before the update. Specifically, the σ-process is defined by the transition rates

$$1 \to 0 \qquad \text{with rate 1} \tag{22}$$

$$10, 01 \to 11 \qquad \text{with rate } q(1 + a/m^\sigma) \tag{23}$$

where m denotes the distance to the next active site. Here a is a constant, q is again the control parameter, and σ is an exponent controlling the characteristics of the interaction. It turns out that for $\sigma > 1$ the transition belongs to the DP universality class, while for $0 < \sigma < 1$ the transition becomes first order.

The model was introduced as a toy model in order to explain why non-equilibrium wetting processes, with a sufficiently strong attractive short range force between interface and substrate, can exhibit a first-order transition. In this case the growth rate in the bulk is positive, with the result that spontaneous pinning far away from the edges can be neglected, meaning that the transition is driven by unpinning and spontaneous growth of bound regions. The binding rate, however, was found to vary with the actual size of the unpinned regions, which motivates the algebraic m-dependent rate in equation (23). It should be noted that the σ-process is mainly relevant for non-equilibrium wetting in one spatial dimension only, where pinned sites effectively separate depinned islands into non-communicating regions. Moreover, there is no unique and straightforward way to extend such a process in higher dimensions. In the following we combine the two long range processes in a single 1D model and study the corresponding phase diagram in the α–σ plane.

3.2. Definition of the α–σ-process

The combined α–σ-model, which evolves by random sequential update over a time step $\mathrm{d}t = 1/L$, is defined by the following transition rates:

$$1 \to 0 \qquad \text{with rate } 1 \tag{24}$$

$$10, 01 \to 11 \qquad \text{with rate } q(1 + a/m^\sigma) \tag{25}$$

$$000 \to 010 \qquad \text{with rate } bq/l^\alpha \tag{26}$$

where m is the size of the inactive island and l denotes the distance from the nearest active site. Here q is the control parameter, α and σ are the control exponents, and a and b are constants. The 'pure' α- and σ-processes are recovered in the limits $\sigma \to \infty$ and $\alpha \to \infty$, respectively.

3.3. Mean field analysis and numerical simulations

Neglecting spatial fluctuations, the mean field equation of the combined α–σ-process (see section 2.1 and [22]) becomes

$$\partial_t \rho = -\rho + q\rho^2 \sum_{m=1}^{\infty} \left(1 + \frac{a}{m^\sigma}\right)(1 - \rho)^m + bq\rho(2 - \rho) \sum_{l=2}^{\infty} \frac{(1-\rho)^{2l-1}}{l^\alpha}. \tag{27}$$

In the regime of interest, namely for $0 < \sigma < 1$ and $1 < \alpha < 2$, the mean field equation can be written to leading order as

$$\partial_t \rho = r\rho + p\rho^{1+\sigma} - u\rho^\alpha + 0(\rho^2), \tag{28}$$

where r, p and u are q-dependent constants:

$$r = q - 1 + bq\frac{2^{2-\alpha}}{\alpha - 1}, \tag{29}$$

$$p = aq\,\Gamma(1 - \sigma), \tag{30}$$

$$u = bq\,\frac{2^{\alpha-1}}{\alpha - 1}\Gamma(2 - \alpha). \tag{31}$$

Note that these are approximate expressions, as they are obtained by replacing the sums in (27) by integrals to obtain simple analytic expressions. This approximation does not affect the signs of p and u which turn out to be positive constants in the regime of interest. Accordingly, if the leading non-linear term is $\rho^{1+\sigma}$ (i.e. $\sigma < \alpha - 1$), the transition is first order. On the other hand, if the leading non-linear term is ρ^α ($\sigma > \alpha - 1$), the critical behaviour of the pure α-model is recovered. Thus, the mean field approach predicts that the critical exponents are independent of σ. One can add the effect of the long range processes on the diffusion constant as was done in section 2.1. It is readily seen that the critical exponent z assumes its DP value for $\alpha > 3$ as long as $\sigma > 1$.
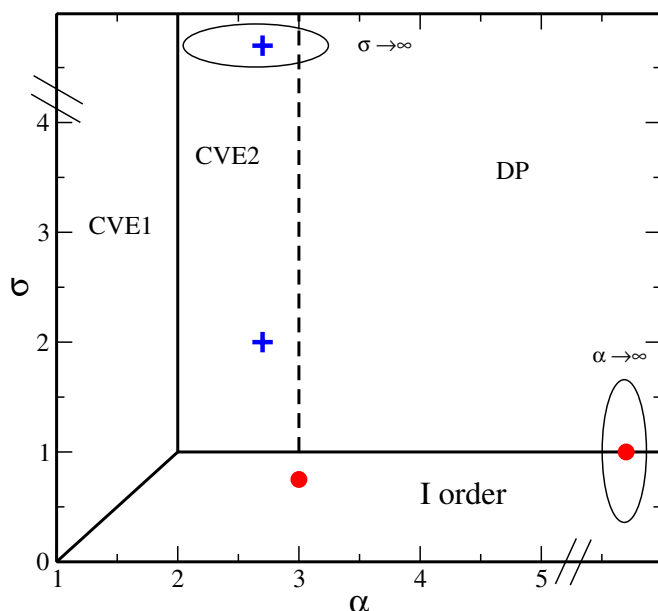
11

Figure 4. Mean field phase diagram of the α–σ-process. Four different regions are identified corresponding to different types of transitions to the absorbing state: a DP region, a region of a first-order transition and two regions of continuously varying critical exponents as explained in the text. We also indicate the phase boundary lines as determined by numerical simulations: full dots for the DP–first-order boundary and crosses for the DP–CVE boundary. The numerical results suggest the existence of a single CVE phase with a single DP–CVE line located at $\bar{\alpha} \approx 2.7$.

The mean field phase diagram is shown in figure 4. It contains four different phases:

(i) A DP phase for $\sigma > 1, \alpha > 3$.

(ii) A continuously varying exponent phase CVE1 for $\sigma > \alpha - 1$ and $1 < \alpha < 2$ where the transition is second order with continuously varying exponents β, δ and z.

(iii) A continuously varying exponent phase CVE2 for $\sigma > 1$ and $2 < \alpha < 3$ where the transition is second order but where z is the only continuously varying exponent.

(iv) A phase for $\sigma < \alpha - 1$ and $0 < \sigma < 1$ where the transition is discontinuous.

Numerical simulations have been performed for testing the predictions of the mean field phase diagram. In these simulations we have taken $a = 2$ and $b = 1$.

An extensive numerical study of the phase diagram of the α–σ-process is time-consuming and was not tackled in the present paper. Rather, we restricted our analysis to a small number of cuts in the α–σ plane in order to test the validity of the mean field predictions. We find that while the general features of the phase diagram are correctly reproduced by the mean field approach, the location of the transition lines and the values of the critical exponents are changed.

The numerical method proposed in [21] has been applied for the inspection of the phase diagram along the line $\sigma = 2$ for a discrete set of values of α ranging between 2 and 3. In these simulations we have used the same system sizes and conditions as are described

Table 2. α–σ-process: estimates of the critical points and exponents for $\sigma = 2$ and various values of α. Other parameters have been fixed at $a = 2$ and $b = 1$.

α	2.0	2.3	2.5	2.6	2.7	3.0
q_c	0.7783(2)	0.9308(3)	1.0155(3)	1.0530(3)	1.0880(5)	1.1785(5)
z	1.18(3)	1.40(3)	1.51(3)	1.50(4)	1.54(5)	1.57(3)
δ	0.32(2)	0.22(1)	0.19(1)	1.18(1)	1.18(1)	1.16(1)
β	0.52(1)	0.37(3)	0.32(3)	0.30(2)	0.29(1)	0.28(2)

in the caption of figure 2. The numerical simulations suggest that in fact there is a single phase with continuously varying exponents (CVE) rather than two as predicted by the mean field approach. In this phase all critical exponents are continuously varying with α. In the DP and CVE regions the critical exponents coincide, within numerical accuracy, with those found for the pure α-model (i.e., $\sigma \to \infty$). The results reported in table 2 are in agreement with the mean field prediction that scaling properties in the critical regions are independent of the σ-process. It is worth stressing that even for finite values of σ the boundary between the DP and the CVE region is located close to $\bar{\alpha} \approx 2.7$. The position of the boundary line for $\sigma = \infty$ and $\sigma = 2$ is marked by crosses on the phase diagram (see figure 4).

We now consider the boundary between the first-order and the DP regions. For the pure σ-model (i.e., $\alpha \to \infty$) this boundary was investigated numerically in [22]. Following [22] we determine the nature of the phase transition for finite α by studying the size distribution of inactive domains in the stationary active state. At the transition to the absorbing state this distribution is expected to exhibit a power-law tail $P(m) \sim m^{-\gamma}$ for large inactive domains of size m. By numerically determining the exponent γ, the nature of the transition may be deduced. For $\gamma > 2$ the average domain size is finite at the transition and thus it is first order. On the other hand for $\gamma \le 2$ the average domain size diverges at the transition and thus the transition is continuous. In particular, for DP, where the transition is continuous, one has $\gamma^{\mathrm{DP}} = 2 - \beta/\nu_\perp \simeq 1.747$.

We have analysed the nature of the phase transition for $\alpha = 3$ at some values of σ ranging between 0.5 and 2. We find that $\gamma = \gamma^{\mathrm{DP}}$ for $\sigma > 0.8$ indicating that the transition to the absorbing state is of DP nature. On the other hand for $\sigma < 0.8$ we find $\gamma > 2$, indicating a first-order transition. The position of the boundary line for $\alpha = \infty$ and $\alpha = 3$ is marked by dots on the phase diagram (see figure 4).

Details of the numerical analysis are presented in figure 5. In this figure we first illustrate the method for identifying the transition point. This is done by plotting $\rho(t)t^{\delta_{\mathrm{DP}}}$ as a function of t for different values of q and searching for the q value for which this quantity approaches a constant. The data were obtained for quite large system sizes ($L \approx 2^{18}$–2^{19}) and homogeneous initial conditions. We then display the distribution function $P(m)$ at the transition, and determine the exponent γ which controls its large m behaviour. The value of the control parameter q at the transition point is given in table 3 for $\alpha = 3$ and several values of the parameter σ.

Our numerical results suggest that the boundary between first-order and DP like behaviour varies with α. In particular it takes place at $\sigma \simeq 0.8$ for $\alpha = 3$ while it is at $\sigma \simeq 1$ in the limit of infinite α. Thus the boundary line in the α–σ plane is not parallel to the α axis, at variance with the mean field prediction.
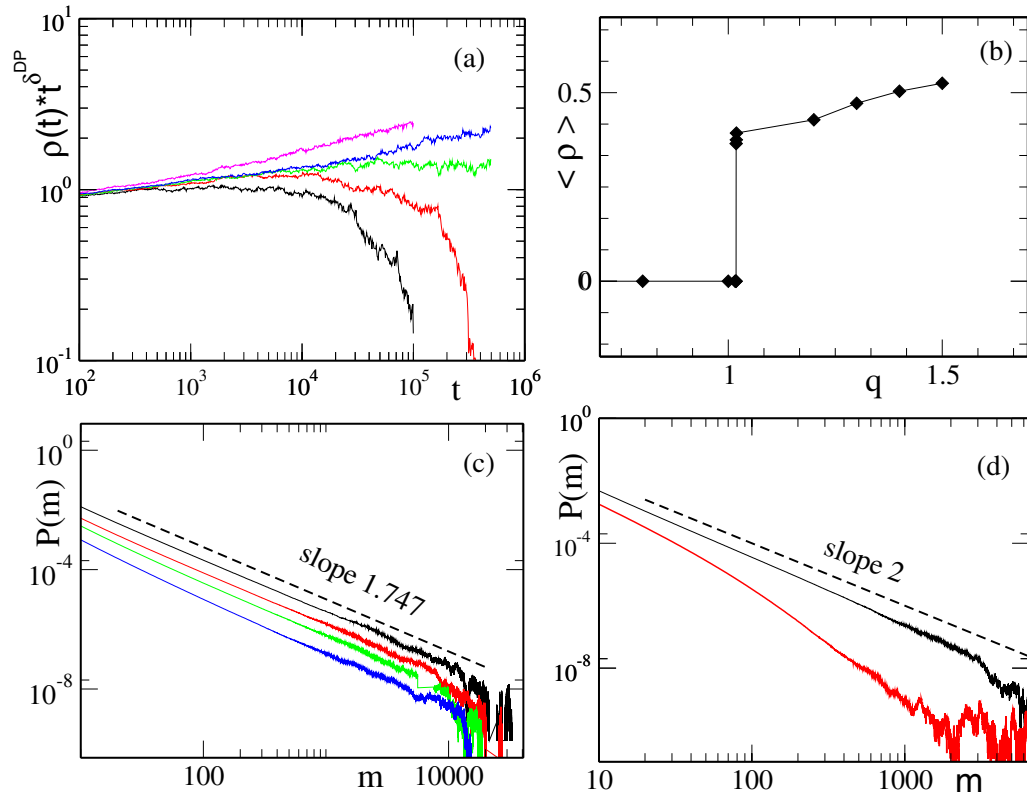
Figure 5. Numerical study of the α–σ-process for $\alpha = 3.0$. (a) $\rho(t)t^{\delta^{\mathrm{DP}}}$ versus t for $\sigma = 0.8$ and values of the control parameter close to $q_c \approx 1.043$: from top to bottom $q = 1.045, 1.044, 1.043, 1.042, 1040$. (b) Stationary density ρ_{stat} as a function of q for $\sigma = 0.7$: a jump occurs at the first-order transition point $q_c \approx 1.0184$. In (c) and (d) we display the probability distribution of the size of inactive domains $P(m)$ at the transition. (c) From top to bottom $\sigma = 1.5, 1.1, 0.9, 0.8$: the power-law decay agrees with the DP scaling (see the dashed line). (d) From top to bottom $\sigma = 0.7, 0.5$: $P(m)$ decays faster then m^{-2} so $\langle m \rangle$ is finite. In both of these plots the curves are not normalized and they have been rescaled to fit on the same plot.

Table 3. α–σ-process: estimates of the critical points q_c for $\alpha = 3$, $a = 2$, $b = 1$ and various values of σ.

σ	0.5	0.7	0.8	0.9	1.1	1.5
q_c	0.9515(5)	1.0184(1)	1.0430(5)	1.0647(3)	1.0992(1)	1.1445(5)

4. Conclusions

In many cases it is useful to project complex dynamical processes onto simpler ones which could be more readily analysed. In doing so it may happen that the local dynamics of the original model is translated into a non-local dynamics of the projected model. For example it has been argued that when the dynamics of fluctuating interfaces interacting

with a wall is projected onto the dynamics of a contact process, different types of long range processes may take place.

Motivated by this observation we introduced a non-local version of the contact process where particles are created with a rate which decays like $l^{-\alpha}$ with the distance l from the nearest particle. Mean field analysis shows that the critical exponent β associated with the transition to the absorbing state varies continuously with α for $1 < \alpha < 2$ and it diverges for α approaching 1. The usual short range mean field exponent $\beta = 1$ is recovered above the threshold $\alpha = 2$. The exponent $\nu_\parallel$ is found to be 1 over the entire range. Numerical studies in one dimension support this general behaviour, although the value of β and the upper threshold seem to be different.

Including spatial fluctuations in the mean field equations, the mean field exponents $\nu_\perp$ and z are evaluated. It is found that near $\alpha = 1$ the exponent z vanishes linearly, while it approaches the usual mean field value $z = 2$ at another threshold, which in one dimension is $\alpha = 3$. Also in this case we find a qualitative agreement with numerics. Extension of the model to include another long range dynamical process, the σ-process, has also been considered using both mean field approximation and numerical simulations. Here, too, the global features of the mean field phase diagram are qualitatively recovered by the numerical study.

Acknowledgments

References

[1] Mollison D, 1977 *J. R. Stat. Soc.* B **39** 283
[2] Liggett T M, 1985 *Interacting Particle Systems* (Heidelberg: Springer)
[3] Marrow J and Dickman R, 1999 *Nonequilibrium Phase Transitions in Lattice Models* (Cambridge: Cambridge University Press)
[4] Hinrichsen H, 2000 *Adv. Phys.* **49** 815
[5] Ódor G, 2004 *Rev. Mod. Phys.* **76** 663
[6] Lübeck S, 2004 *Int. J. Mod. Phys.* B **18** 3977
[7] Alon U, Evans M R, Hinrichsen H and Mukamel D, 1996 *Phys. Rev. Lett.* **76** 2746
    Hinrichsen H, Livi R, Mukamel D and Politi A, 1997 *Phys. Rev. Lett.* **79** 2710
    Hinrichsen H, Livi R, Mukamel D and Politi A, 2000 *Phys. Rev.* E **61** R1032
    Hinrichsen H, Livi R, Mukamel D and Politi A, 2003 *Phys. Rev.* E **68** 041606
[8] Giada L and Marsili M, 2000 *Phys. Rev.* E **62** 6015
[9] Candia J and Albano E V, 2000 *Eur. J. Phys.* B **16** 531
[10] de los Santos F, da Gama M M T and Muñoz M A, 2002 *Europhys. Lett.* **57** 803
     de los Santos F, da Gama M M T and Muñoz M A, 2003 *Phys. Rev.* E **67** 021607
[11] Kissinger T, Kotowicz A, Kurz O, Ginelli F and Hinrichsen H, 2005 *J. Stat. Mech.* P06002
[12] Marques M C and Ferreira A L, 1994 *J. Phys. A: Math. Gen.* **27** 3389
[13] Albano E V, 1996 *Europhys. Lett.* **34** 97
[14] Bouchaud J P and Georges A, 1990 *Phys. Rep.* **195** 127
[15] Janssen H K, Oerding K, van Wijland F and Hilhorst H J, 1999 *Eur. Phys. J.* B **7** 137
[16] Hinrichsen H and Howard M J, 1999 *Eur. Phys. J.* B **7** 635
[17] Jiménez-Dalmaroni A, 2006 *Preprint* cond-mat/0603151

[18] Adamek J, Keller M, Senftleben A and Hinrichsen H, 2005 *J. Stat. Mech.* P09002
[19] Brockmann D and Geisel T, 2003 *Phys. Rev. Lett.* **90** 170601
[20] Jensen I, 1999 *J. Phys. A: Math. Gen.* **32** 5233
[21] de Oliveira M M and Dickman R, 2005 *Phys. Rev.* E **71** 016129
    Dickman R and de Oliveira M M, 2005 *Physica* A **357** 134
[22] Ginelli F, Hinrichsen H, Livi R, Mukamel D and Politi A, 2005 *Phys. Rev.* E **71** 026121